1 **Identification of Benzo[a]pyrene(BaP)-Metabolizing Bacteria in Forest Soils**
2 **Using DNA-Based Stable-Isotope Probing**

3

4 Mengke Song [1], Chunling Luo [1 *], Longfei Jiang [1], Dayi Zhang [2], Yujie Wang [3], Gan
5 Zhang [1]

6

7 [1] Guangzhou Institute of Geochemistry, Chinese Academy of Sciences, Guangzhou 510640, China
8 [2] Lancaster Environment Centre, Lancaster University, Lancaster LA1 4YQ, UK
9 [3] School of Environmental Science and Engineering, Guangdong University of Technology,
10 Guangzhou 510006, China
11 * Corresponding author: Dr. Chunling Luo
12 E-mail: clluo@gig.ac.cn; Tel.: +86-20-85290290; Fax: +86-20-85290706

13

14 **Running Title:** BaP Degraders Examined with SIP

15

ABSTRACT

DNA-based stable-isotope probing (DNA-SIP) was used in this study to investigate the uncultivated bacteria with benzo[a]pyrene (BaP) metabolism capacities in two Chinese forest soils (Mt. Maoer in Heilongjiang Province and Mt. Baicaowa in Hubei Province). Three different phylotypes were characterized with responsibility for BaP degradation, none of which was previously reported as BaP-degrading microorganisms by SIP. In Mt. Maoer soil microcosms, the putative BaP degraders were classified as belonging to the genus *Terrimonas* (family *Chitinophagaceae*, order *Sphingobacteriales*), whereas *Burkholderia* were the key BaP degraders in Mt. Baicaowa soils. The addition of metabolic salicylate significantly increased BaP degradation efficiency in Mt. Maoer soils, and the BaP-metabolizing bacteria shifted to the microorganisms in the family *Oxalobacteraceae* (genus unclassified). Meanwhile, salicylate addition did not change either BaP degradation or putative BaP degraders in Mt. Baicaowa. Polycyclic aromatic hydrocarbon-ring hydroxylating dioxygenase (PAH-RHD) genes were amplified, sequenced and quantified in the DNA-SIP ^{13}C heavy fraction to further confirm the BaP metabolism. By discussing the microbial diversity and salicylate additive effects on BaP degradation across different soils, the results increased our understanding of BaP natural attenuation and provided possible approach to enhance the bioremediation of BaP-contaminated soils.

Keywords: stable isotope probing (SIP), benzo[a]pyrene (BaP), forest soil, PAH-RHD gene, salicylate

38

39 **INTRODUCTION**

40 Polycyclic aromatic hydrocarbons (PAHs), a class of persistent organic pollutants
41 (POPs), enter the environment through both natural and anthropogenic pathways.
42 PAHs are released into the environment by means of natural processes such as forest
43 fires and direct biosynthesis under the action of microbes and plants (1). The primary
44 artificial source of PAHs is the incomplete combustion of organic matter at high
45 temperatures caused by human activities (2). Their presence in the environment poses
46 a severe threat to public and ecosystem health because of their known acute toxicity,
47 and mutagenic, teratogenic, and carcinogenic features; they are therefore classified as
48 priority pollutants by the U.S. Environmental Protection Agency (3). Furthermore, the
49 persistence and genotoxicity of PAHs increase with molecular weight, and the
50 presence of high-molecular-weight (HMW) PAHs in the environment is of greater
51 concern. Benzo[a]pyrene (BaP), a representative HMW PAH with a five-ring structure,
52 is a widespread pollutant with potent mutagenic and carcinogenic properties (4, 5).
53 BaP is therefore identified as the first class of "human carcinogens" according to the
54 report of the World Health Organization (WHO) International Agency for Research on
55 Cancer (6). Generally, in soils with no industrial contamination, BaP concentrations
56 vary from 3.5 to 3700 μg/kg, with a median concentration of 16 μg/kg soil; in
57 contaminated soils and sediments, BaP concentrations range from 82 to 536 mg/kg
58 (7).

59 Bacteria possessing the ability of BaP utilization are readily isolated from

60 contaminated soils or sediments, and most of our current knowledge about BaP
61 metabolism by microbes has been gained from such isolates (8-10). The functional
62 PAH-RHD genes (encoding PAH-ring hydroxylating dioxygenase enzymes) have also
63 been examined to understand BaP degradation mechanisms, such as *nah*, *pah*, *arh* and
64 *phn* genes in Gram-negative (GN) bacteria and the evolutionarily correlated *nid*, *nir*,
65 *phd* and *nar* genes in Gram-positive (GP) bacteria, which are responsible for the first
66 step of PAHs (naphthalene, phenanthrene, anthracene and pyrene) hydroxylation
67 under aerobic conditions (11, 12). Terminal dioxygenase is the component of
68 PAH-RHD, composed of large α and small β subunits. The genes coding for the
69 mononuclear iron-containing catalytic domain (a conserved regions) of PAH-RHDα
70 (α-subunit) have been widely used for studying RHD diversity and the
71 PAH-degradation potential by bacteria in environment (11). In addition to the research
72 on the genes involved in PAH degradation, studies using culture-dependent tools to
73 investigate the degrading capacity of BaP degraders showed that rare bacteria were
74 capable of metabolizing BaP without metabolic intermediate additives (9, 10, 13); in
75 most cases, BaP degradation is stimulated by the addition of some intermediates
76 produced during BaP metabolism (14, 15). These intermediates possess the ability of
77 stimulating PAH dioxygenase activity and are capable of supplying electrons for
78 nicotinamide adenine dinucleotide (NADH) coenzymes, which are necessary for the
79 functions of oxygenase enzymes, to initiate aerobic PAH degradation (8, 16).
80 Salicylate is a classic intermediate, inducing PAHs metabolism of PAHs-degrading
81 bacteria and selectively stimulating their growth (8, 16, 17). The addition of salicylate

82 to contaminated soils or sediments has been proposed as a means of encouraging PAH
83 degradation during bioremediation (16). *Sphingomonas yanoikuyae* JAR02 was
84 reported to completely remove BaP (1.2 mg/L) within 20 h in the aqueous phase with
85 additive salicylate (8). Additionally, *Pseudomonas saccharophila* P15 isolated from
86 creosote-contaminated soil improved BaP removal after the addition of salicylate,
87 which acted as the inducer of PAH dioxygenase activity (16).
88 The traditional culture-dependent approaches, such as isolating and cultivating
89 target bacteria in the laboratory, suffer from the fact that <1% of the soil
90 microorganisms are cultivable. The process underestimates the diversity of the
91 prokaryotes and fails to capture the true nature of the complex interactions within
92 microbial communities at a specific site. The uncultured bacteria may possess an
93 unexplored reservoir of novel and valuable gene-encoding catalysts that benefit
94 bioremediation, industry, and medicine (18-20). Furthermore, with our limited
95 understanding of the actual biota, cultivation presents challenges for field
96 bioremediation (21). In recent years, stable-isotope probing (SIP) has emerged as a
97 culture-independent method to identify microorganisms capable of utilizing specific
98 substrates in complex environments. Microbial populations responsible for the
99 degradation of targeted contaminants are labeled by stable isotopes and then
100 characterized (22-25). To date, many bacteria have been successfully identified by SIP
101 with their unique capabilities of metabolizing phenolic compounds and PAHs, such as
102 naphthalene (25, 26), anthracene (27), phenanthrene (26), pyrene (23, 28),
103 fluoranthene (29), benz[a]anthracene (29), biphenyl (30, 31), phenol (31), and

104 benzoate (31). However, to our knowledge, no study till now has examined
105 BaP-degrading bacteria successfully using SIP.

106 In the present study, to investigate the microorganisms responsible for BaP
107 degradation in the uncontaminated soil, ^{13}C-DNA-targeted SIP was applied to two
108 Chinese forest soils from Mt. Maoer and Mt. Baicaowa. The influence of salicylate on
109 BaP biodegradation was further studied, as well as its role in functional microbial
110 community dynamics. By sequencing and quantifying (by real-time polymerase chain
111 reaction, qPCR) PAH-RHDα genes in ^{13}C-DNA enriched fraction, our work further
112 revealed the BaP metabolism in uncontaminated soil and the stimulating effects of
113 salicylate addition varying among different soils. To our knowledge, this study
114 successfully apply the culture-independent SIP technique to characterize
115 BaP-degrading bacteria in forest soil, and provides an important contribution to the
116 understanding of BaP biodegradation in complex communities and the bioremediation
117 of HMW PAHs-contaminated soil.

118

119 **MATERIALS AND METHODS**

120 **Soil samples.** Soil samples were collected from Mt. Maoer (45°22′48″N,
121 127°40′48″E) in Heilongjiang Province, and Mt. Baicaowa (40°48′36″N, 117°35′60″E)
122 in Hebei Province, China. The pH and total organic carbon content were 7.5 and 16.0%
123 (Mt. Maoer), and 6.0 and 12.3% (Mt. Baicaowa), respectively. Before use, large
124 objects in the soils, such as stones and debris, were removed manually in the
125 laboratory. The soil samples were then homogenized, sieved through a 2-mm

126 pore-size screen, and prepared for the BaP-degradation treatment.

127 **Setup of BaP-degrading microcosms.** Both non-salicylate and salicylate-additive
128 treatments were included for the two forest soils. Hereafter, BS and B represent the
129 Mt. Baicaowa soils amended with and without salicylate, and MS and M denote the
130 Mt. Maoer soils amended with and without salicylate, respectively. The experiments
131 were conducted as follows: Three grams of soil (dry weight) was placed in a 150-mL
132 serum bottle containing 10 mL phosphate-buffered mineral medium (32). The bottles
133 were sealed with rubber stoppers and compressed with an aluminum seal. The
134 unlabeled BaP (99%) or ^{13}C-labeled BaP ($^{13}C_4$-BaP, 99%, Fig. S1 shows the position
135 of ^{13}C-labeled carbons), both from Cambridge Isotope Laboratories, Inc. and
136 dissolved in nonane with a final concentration of 100 mg/l, was added to the
137 respective bottles using a gastight syringe to give a final BaP concentration of 1
138 mg/kg. For salicylate-additive treatments, the final salicylate concentration was 10
139 mg/kg. Two negative control treatments were included as no-carbon-source (CK) and
140 non-bioactive (sterilized by γ -irradiation, ^{12}C-NB). Two positive treatments were
141 amended with ^{12}C- and ^{13}C-labeled BaP carbon sources, named as ^{12}C-BT and ^{13}C-BT,
142 respectively. Eight samples were prepared for each treatment. The microcosms were
143 incubated at room temperature (~25 ℃) with reciprocal shaking at a speed of 120
144 rpm/min. On Day 7, 14, 28, and 42 after incubation, two samples from each treatment
145 were sacrificed for BaP analysis and DNA extraction, respectively. All stock solutions
146 were filtered through 0.2-μm pore-size filters and stored in dark-brown containers. To
147 prepare sterile controls, soils were γ-irradiated (50 kGy) for 2 h before use.

148 **BaP analysis.** The ^{12}C-NB, ^{12}C-BT and ^{13}C-BT samples were prepared for BaP
149 analysis using the following steps: The serum bottles were frozen at -20 ℃ overnight,
150 followed by freeze-drying using a vacuum freeze dryer. The dry soil samples were
151 then homogenized, pulverized, spiked with 1,000 ng of deuterated PAHs as surrogate
152 standards and extracted with dichloromethane (DCM) in a Soxhlet apparatus for 48 h,
153 with the addition of activated copper to remove sulfur. The extract was concentrated
154 to ~0.5 mL after solvent exchange to hexane. The soil extracts were purified in a
155 multilayer silica gel/alumina column (8 mm i.d.) filled with anhydrous Na_2SO_4 (1 cm),
156 neutral silica gel (3 cm, 3% w/w; deactivated), and neutral alumina (3 cm, 3% w/w;
157 deactivated; from top to bottom) via elution with 15 mL hexane/DCM (1:1, v/v). After
158 concentrating to ~50 μL under a gentle stream of N_2, 1,000 ng of hexamethylbenzene
159 was added as an internal standard prior to analysis.

160 BaP was detected on an Agilent 7890 gas chromatograph equipped with a
161 capillary column (DB-5MS, 30 m, 0.25 mm, 0.25 μm) and a mass spectrometric
162 detector (MSD, Agilent 5975). One microliter of sample was injected in splitless
163 mode with a 10-min solvent delay time. High-purity helium was used as the carrier
164 gas at a flow rate of 1.83 mL/min. The temperature of the injector and transfer lines
165 was 290 and 300 ℃, respectively. The initial oven temperature was set at 60 ℃ for 1
166 min, rising to 290 ℃ at a rate of 3 ℃/min, and was subsequently held constant for 20
167 min. PAH standards were used to quantify BaP. Instrumental performance was
168 subjected to quality-control calibration with the standards after each set of eight
169 samples had been analyzed. Six PAHs standard concentrations were used to derive the

170 calibration curves. Concentrations were corrected using reference to surrogate
171 recovery levels.

172 **DNA extraction and ultracentrifugation.** Samples from ^{12}C-BT and ^{13}C-BT
173 were both prepared for biotic analysis at 7, 14, 28, and 42 days of cultivation. The
174 total genomic DNA was extracted from 1.0 g soils with triplicates using the
175 Powersoil® DNA Isolation Kit (MO BIO Laboratories, Inc.) according to the
176 manufacturer's protocol. DNA concentrations were determined using an ND-2000
177 UV-Vis spectrophotometer (NanoDrop Technologies). Subsequently, ~10,000 ng
178 DNA was added to Quick-Seal polyallomer tubes (13 × 51 mm, 5.1 mL, Beckman
179 Coulter), along with a Tris-EDTA (TE, pH 8.0)/cesium chloride (CsCl) solution.
180 Before the tubes were sealed with cordless Quick-Seal® Tube Topper (Beckman
181 Coulter), the average buoyant density (BD) of all prepared gradients was determined
182 with an AR200 digital refractometer (Leica Microsystems Inc.) and adjusted to ~1.77
183 g/mL by adding a CsCl solution or Tris–EDTA buffer, if necessary. The tubes were
184 transferred to an ultracentrifuge (Optima L-100XP, Beckman Coulter) and centrifuged
185 at 178,000 × *g* (20 ℃) for 48 h. Following centrifugation, 150-μL fractions were
186 collected from each tube using a fraction recovery system (Beckman Coulter). The
187 BD of each fraction was measured, and the CsCl was further removed by
188 glycogen-assisted ethanol precipitation (33).

189 **PCR and terminal restriction fragment length polymorphism (TRFLP).** The
190 fractions were subjected to terminal restriction fragment length polymorphism
191 (TRFLP) analysis using standard procedures (24). Briefly, DNA was amplified with

192 27F-FAM (5′-AGAGTTTGATCMTGGCTCAG; 5′ end-labeled with
193 carboxyfluorescein) and 1492R (5′-GGTTACCTTGTTACGACTT) using the
194 following PCR program: initial melting at 94 ℃ for 5 min, 30 amplification cycles at
195 94 ℃ for 30 s, 55 ℃ for 30 s, and 72 ℃ for 1.5 min, with a final extension at 72 ℃ for
196 10 min. After amplification, the presence of PCR products was confirmed by 1%
197 agarose gel electrophoresis. The PCR products were purified using an EZNA
198 Cycle-Pure Kit (Omega Bio-Tek, Inc.) following the manufacturer's instructions and
199 digested with *Hae*III (New England Biolabs) for 4–5 h at 37 ℃. One nanogram of
200 each labeled PCR product was analyzed on an ABI 3730 Genetic Analyzer (Applied
201 Biosystems) running Peak Scanner software version 1.0 (Applied Biosystems). A
202 GeneScan™ ROX 500™ set of internal standards (Applied Biosystems) was used.
203 The percent abundance of each fragment was determined as previously described
204 (30).

205 **Identification of the PAH-RHDα gene in microcosms and enumeration in SIP**
206 **fractions.** As the PAH-RHDα genes possessed by GN and GP bacteria do not belong
207 to a monophyletic cluster (12), the presence of the PAH-RHDα genes was
208 investigated using PAH-RHDα GP primers (641F
209 5'-CGGCGCCGACAAYTTYGTNGG, 933R
210 5'-GGGGAACACGGTGCCRTGDATRAA) and PAH-RHDα GN primers (610F
211 5'-GAGATGCATACCACGTKGGTTGGA, 911R 5'-
212 AGCTGTTGTTCGGGAAGAYWGTGCMGTT) (32) on the heavy DNA fractions
213 from B, BS, M and MS microcosms, respectively. A gradient PCR was performed

214 with annealing temperatures ranging from 52 to 62 ℃. Amplification reactions were

215 carried out in a volume of 50 μL, as previously described (12).

216 The copy number of the PAH-RHDα sequences in fractions from ^{13}C-labeled and

217 unlabeled DNA was determined by qPCR using the PAH-RHDα GP primers, because

218 only one strong and specific amplicon amplified with PAH-RHDα GP primers was

219 produced from the heavy fractions in M and MS microcosms in this work. The PCR

220 mix contained 10 μL SYBR Green® PCR Premix Ex Taq^{TM} II (TaKaRa Bio) and 1 μL

221 DNA template in a final volume of 20 μL. A standard curve was obtained by

222 producing 10 dilution series of plasmid pGEM-T Easy Vector sequences (10^2–10^8

223 copies; Promega) containing the PAH-RHDα gene detected in M and MS treatments

224 with the PAH-RHDα GP primers (641F 5'-CGGCGCCGACAAYTTYGTNGG, 933R

225 5'-GGGGAACACGGTGCCRTGDATRAA). The amplification reactions were

226 conducted using a two-step method in a 48-well optical plate on an Eco^{TM} real-time

227 PCR system (Illumina) as follows: denaturation for 10 min at 95 ℃, followed by 40

228 cycles of 10 s at 95 ℃, and 30 s at 60 ℃; then the SYBR Green signal intensities were

229 measured after the 30 s step at 60 ℃. At the end of the real-time PCR, a melting curve

230 analysis was performed by increasing the temperature from 55 to 95 ℃. For each

231 DNA sample, the average of three replicates was determined as the copy number per

232 fraction.

233 **Sequencing of partial PAH-RHDα and 16S rRNA genes.** The 16S rRNA genes

234 from the heavy fractions (^{13}C-labeled DNA, marked with ☆ in Fig. 1)

235 corresponding to the peak in Fig. 1A- Fig. 1D with the BD value of 1.7198 g/ml,

236 1.7203 g/ml, 1.7165 g/ml and 1.7100 g/ml, as well as the amplicons generated with
237 the PAH-RHDα GP primer pair in M and MS treatments, were cloned and sequenced.
238 Briefly, the 16S rRNA gene was amplified using a similar process to that described
239 above, except the 27F-FAM primer was replaced by 27F. The purified PCR products
240 were cloned into a pGEM-T Easy Vector and transformed into *Escherichia coli* JM
241 109 (TaKaRa Bio). *E. coli* clones were then grown on Luria-Bertani medium
242 solidified with 15 g/L agar in the presence of 50 μg/L ampicillin for 16 h at 37°C, and
243 finally 100 clones with inserts were selected to be sequenced. The plasmids with
244 target genes were extracted using an EZNA Plasmid Mini-Kit (Omega Bio-Tek, Inc.),
245 and the recombinants were selected using 0.8% agarose gel electrophoresis and
246 sequenced on an ABI 3730 genetic analyzer using M13 primers. Sequence similarity
247 searches and alignments were performed using the Basic Local Alignment Search
248 Tool (BLAST) algorithm (National Center for Biotechnology Information) and
249 Molecular Evolutionary Genetics Analysis (MEGA 5.1).
250 The obtained 16S rRNA gene and the partial RHD gene sequences are available in
251 GenBank (accession numbers KM267480–KM267482 for partial 16S rRNA gene
252 sequences of a 196-bp terminal restriction fragment (TRF) in B and BS treatments,
253 450-bp TRF in M treatment, and 216-bp TRF in MS treatment; KM267486 was used
254 for the partial PAH-RHDα gene sequence).
255
256 **RESULTS**
257 **BaP biodegradation in soils.** BaP biodegradation in the four treatments (B, BS,

258 M and MS) is briefly listed in Table 1. The recovery rates of BaP during the extraction
259 procedure were 80%-90% in this work (Table S2). The BaP concentration in sterile
260 treatments showed less decline comparing to unsterilized treatments. For instance, the
261 residual BaP were 80.6%, 72.6%, 81.0% and 69.7% for the ^{12}C-NB of B, BS, M and
262 MS microcosms, respectively. Significant BaP biodegradation was observed in the
263 unsterilized microcosms. For B and BS treatments (Table 1), BaP degradation
264 achieved 16.6% and 18.1% respectively after 7 days cultivation, and 33.4% and 31.1%
265 of BaP was removed after 28 days. No significant BaP degradation difference was
266 found between the B and BS treatments throughout the whole process, indicating the
267 limited impacts of salicylate on the capacities of BaP-degrading bacteria. The BaP
268 degradation in M and MS treatments was much faster than those from Mt. Baicaowa.
269 For example, 32.1% and 47.4% of BaP was removed in M and MS samples after 14
270 days cultivation, compared to the corresponding degradation efficiency of 24.9% and
271 23.0% in B and BS samples. Salicylate significantly accelerated BaP biodegradation
272 in soils from Mt. Maoer, where BaP removal efficiency was 32.1%, 43.7%, and 45.7%
273 in M treatments at 14, 28, and 42 days, compared to the corresponding 47.4%, 52.5%,
274 and 55.8% in MS treatments (Table 1).

275 **Microbial structure analysis via SIP and TRFLP.** DNA extracts from ^{12}C-BT
276 and ^{13}C-BT soil samples were subjected to ultracentrifugation and fractionation,
277 followed by TRFLP for each fraction. The organisms responsible for ^{13}C assimilation
278 were detected by the relative abundances of specific TRFs between the control
279 (^{12}C-BT) and the treatment with ^{13}C-labeled BaP (^{13}C-BT) at all three sampling points

280 for each fraction.

281 In B microcosms, the TRFLP results (Fig. 1) indicated that the 196-bp *Hae*III TRF
282 at higher buoyant densities (1.7176–1.7328 g/mL) was enriched at 7, 14, and 28 days
283 (16.6%, 24.9%, and 33.4% BaP removal, respectively) in ^{13}C-BT samples and that its
284 relative abundance increased with time. Such enrichment and increasing trend were
285 not observed in the ^{12}C-BT controls. Additionally, the enrichment of the 196-bp
286 *Hae*III TRF in the heavy fractions was also supported by their higher fluorescence
287 intensity in the 28-day treatments (Fig. S2A), suggesting that ^{13}C was incorporated by
288 the microorganisms represented by the 196-bp *Hae*III TRF. To identify the
289 BaP-degrading bacteria and obtain the phylogenetic affiliation of the 196-bp *Hae*III
290 TRF, the 16S rRNA clone library derived from the ^{13}C heavy fractions was sequenced,
291 and the clones with the 193-bp *Hae*III TRF cut site matched the TRFLP results for the
292 196-bp TRFs. The slight difference (2–3 bases) between the measured fragment
293 lengths and those predicted using sequence data has been noted in previous studies
294 (24, 34, 35). Based on the comparative analyses of 16S rRNA, the bacteria
295 represented by the 196-bp TRF were classified as members of the genus *Burkholderia*
296 (Fig. S3). Additionally, a partial sequence with the predicted 213-bp *Hae*III cut site in
297 the clone library was related to the class *Acidobacteria*. An additional member with
298 the predicted 206-bp *Hae*III cut site in the clone library was related to the genus
299 *Rhodanobacter* (Table S1).

300 In BS microcosms with salicylate addition, the bacteria represented by the 196-bp
301 *Hae*III TRF were involved in BaP biodegradation, as shown by DNA-SIP. Fig. 1A

302 illustrates a clear increasing relative abundance of 196-bp *Hae*III TRF at higher BD
303 (>1.7203 g/mL) in the ^{13}C-BT samples compared to the ^{12}C-BT at 7, 14, and 28 days.
304 Furthermore, in the ^{13}C-BT samples after 28 days cultivation, the BD value of the
305 strongest fluorescence intensity of the 196-bp *Hae*III TRF was higher than that of the
306 ^{12}C-BT samples (Fig. S2B). When the 16S rRNA clone library derived from the ^{13}C
307 heavy fractions was inspected (Table S1), 43 of the 100 clones with the predicted
308 193-bp *Hae*III cut site fell in the genus *Burkholderiales*. These clones were associated
309 with BaP degradation, the same as the BaP degraders in B treatment. Additionally,
310 three different clones with the predicted 362-, 217-, and 202-bp *Hae*III cut sites were
311 classified within the order *Burkholderiales*, and one clone with the predicted 212-bp
312 *Hae*III cut site shared 100% similarity with strain *Acidobacteria* Gp3, which also
313 occurred in the heavy fraction of B treatment.

314 In M microcosms, the TRFLP fraction profiles (Fig. 1C) and the fluorescence
315 intensity at 42 days (Fig. S2C) indicated relatively more abundant 450-bp *Hae*III TRF
316 in the heavy fractions (BD >1.7121 g/mL) of ^{13}C-BT samples, but not in ^{12}C-BT
317 samples. Furthermore, the relative abundance of the 450-bp *Hae*III TRF in the heavy
318 fraction increased with time in ^{13}C-BT samples, and the magnitude of the increase
319 was largest for the sample that had been left the longest. For the ^{12}C-BT samples, the
320 increase occurred in the light fraction (BD <1.7045 g/mL), indicating ^{13}C-BaP
321 assimilation by the bacteria represented by the 450-bp *Hae*III TRF. However, this was
322 not the dominant TRFLP fragment in the heavy fractions from ^{13}C-BT samples, and
323 the other three TRFs (237, 372, and 215 bp) were the major members. Nevertheless,

324 those microorganisms were not responsible for ^{13}C-BaP degradation since a similar
325 abundance was found in the heavy fractions of the ^{12}C-BT samples. The sequence of
326 16S rRNA clone libraries with the predicted 447-bp cut site fit well with the TRFLP
327 results. They were assigned to the genus *Terrimonas* (phylum *Bacteroidetes*, class
328 *Sphingobacteria*, order *Sphingobacteriales*, family *Chitinophagaceae*), belonging
329 most closely to the *Flavisolibacter ginsengiterrae* strain Gsoil 492 (Fig. S4). Three
330 clones with predicted 237-, 372-, and 215-bp *Hae*III cut sites also appeared in the 16S
331 rRNA clone library derived from the ^{13}C heavy fractions (Table S1), and they were
332 classified in the genus *Spartobacteria incertae sedis*, class *Acidobacteriaceae* and
333 family *Oxalobacteraceae*, respectively.

334 In MS treatment with salicylate addition, the 216-bp *Hae*III TRF was involved in
335 the BaP biodegradation, and was enriched as the dominant TRF in the heavy fractions
336 (BD >1.7056 g/mL) at 28 and 42 days (Fig. 1D and Fig. S2D). An increasing relative
337 abundance was also observed for 14–42 days of cultivation in treatments amended
338 with ^{13}C-BaP, but not in ^{12}C-BT samples (Fig. 1D). Such increase suggested that
339 microorganisms represented by the 216-bp TRF were responsible for ^{13}C substrate
340 uptake (^{13}C-BaP degradation). Additionally, the relative abundance and fluorescence
341 intensity of the 77-, 200-, and 450-bp TRFs (Fig. S2D) were also high in the heavy
342 fractions, but lower than the 216-bp TRF in the ^{13}C-BT samples. The BD values of the
343 three TRFs and their trends of relative abundance were similar between ^{13}C-BT and
344 ^{12}C-BT treatments at the three sampling times. Hence, the microorganisms
345 represented by the three TRFs were not directly involved in BaP degradation, and the

346 large proportion of TRFs in the fractions might be due to their tolerance to BaP.
347 Clones with the 216-bp *Hae*III cut site from 16S rRNA clone libraries matched the
348 TRFLP results, classified as members of the family *Oxalobacteraceae* (phylum
349 *Proteobacteria*, class *Betaproteobacteria*, order *Burkholderiales*) , also present in
350 MS ^{13}C-BaP treatment, and sharing 98% sequence similarity with *Janthinobacterium*
351 *lividum* strain DSM 1522 (Fig. S5). Clones with 77-, 200-, and 447-bp *Hae*III cut sites
352 were classified in the order *Actinomycetales*, family *Burkholderiaceae*, and genus
353 *Terrimonas*, respectively (Table S1-MS).

354 **Occurrence and quantification of PAH-RHDα genes in the SIP fractions.** In B,
355 BS, M, and MS treatments, PAH-RHDα GP amplicons were only detected in the
356 heavy fractions from the ^{13}C-BaP-amended M and MS microcosms with the primer
357 pair of 641f and 933r (Fig. 2), although both PAH-RHDα GP and PAH-RHDα GN
358 primers were used to amplify PAH-RHDα genes in all treatments. In both treatments,
359 the PAH-RHDα gene (PAH-RHDα-M) sequences shared 99% similarity with those of
360 an uncultured strain (KF656719.1), and also high sequence similarity with the
361 affiliation to the genus *Mycobacterium* which was capable of degrading BaP (15, 36).
362 Recently, the microbial metabolism of low-molecular-weight (LMW) PAHs with no
363 more than three rings has been studied extensively, including their metabolic
364 pathways, and enzymatic and genetic regulation (7). However, little is known about
365 the metabolic pathways and genes related to BaP degradation and other HMW-PAHs
366 (37). Therefore, not all the functional genes derived from the active BaP-degrading
367 bacteria could be detected by the primer sets used in this study.

368 PAH-RHDα-M genes in M and MS treatments were quantified against each
369 density-resolved fraction (Fig. 3). A marked enrichment of PAH-RHDα-M genes in
370 the heavy fractions (BD >1.7200 g/mL) was observed in the ^{13}C-BaP-amended soils
371 in MS treatment, indicating that the BD value of PAH-RHDα-M increased with
372 ^{13}C-BaP degradation efficiency. In ^{12}C-BaP control, the majority of the
373 PAH-RHDα-M genes were found in fractions with BD <1.7200 g/mL (Fig. 3A). For
374 M treatment, no significant difference was observed between the ^{13}C-BT and ^{12}C-BT
375 samples due to the limited changes in the PAH-RHDα-M genes and BD value (Fig.
376 3B). Hence, the detected PAH-RHDα-M genes were associated with BaP degradation
377 in MS but not in M treatment, attributing to the salicylate addition, which
378 significantly promoted the expression of PAH-RHDα-M genes, stimulated
379 PAH-RHDα-M encoding bacteria and improved BaP biodegradation.
380
381 **DISCUSSION**
382 **Microorganisms responsible for the BaP degradation.** DNA-SIP has been
383 widely applied to the identification of pollutant degraders in numerous environmental
384 media and with an ever-expanding pool of compounds (22, 27, 38). In the present
385 study, the coupling of DNA-SIP and TRFLP techniques revealed the bacteria
386 correlated with BaP metabolism in soils from Mt. Maoer and Mt. Baicaowa. Bacteria
387 represented by 196-bp TRF were classified as members of the genus *Burkholderia*,
388 and involved in BaP degradation in both B and BS treatments. *Burkholderia*-related
389 bacteria have been linked with PAHs (39) and biphenyl (40) biodegradation in soil.

390 As the dominant genus with key roles in the degradation of oil components (41),
391 *Burkholderia* was found to be capable of degrading anthracene, phenanthrene,
392 chrysene, and pyrene (7). Juhasz et al. found that a *Burkholderia cepacia* strain
393 isolated from soil near a manufacturing gas plant could degrade BaP with pyrene as
394 the carbon source, although only 1.4–6.2% BaP was removed after 56 days (42). A
395 *Delftia* strain was isolated from the microbial consortium of a crude oil-contaminated
396 soil and removed 56.6% BaP in PAH-contaminated soil after 14 days (43). To our
397 knowledge, prior to this study, BaP degradation by *Burkholderia*-related
398 microorganisms using DNA-SIP has not been documented.

399 In M treatment, microorganisms represented by the 450-bp TRF were correlated
400 with BaP degradation and assigned to the genus *Terrimonas*. Sequence analysis
401 suggested their close relationship to the *F. ginsengiterrae* strain Gsoil 492 (Fig. S4).
402 This strain was first isolated by Yoon and Im from soil used for ginseng planting, and
403 it has the ability for growth with 3-hydroxybenzoic or 4-hydroxybenzoic acid as the
404 sole carbon source (44). Strains of the genus *Sphingomonas* from the family
405 *Sphingomonadaceae*, order *Sphingomonadales*, were able to degrade BaP with
406 different co-metabolic substances, and aqueous 1.2 mg/L BaP was completely
407 removed within 20 h when *S. yanoikuyae* JAR02 grew on salicylate (8). Ye et al. also
408 showed that 5% BaP was removed by *Sphingomonas paucimobilis* with fluoranthene
409 as the co-metabolic source of carbon and energy after 168 h when the initial
410 concentration of BaP was 10 mg/L (45). Until now, some strains affiliated to
411 *Chitinophagaceae* were found in various environments and possessed the functions of

412 metabolizing complex organic compounds. Though the crucial roles of these strains in
413 carbon circulation were reported (46), little was known about their PAH-degrading
414 capabilities. The present study show that the genus *Terrimonas* correlated with BaP
415 degradation, which expand our knowledge of this genus.

416 The bacteria involved in BaP degradation in MS microcosm amended with BaP
417 and salicylate were affiliated most closely with the family *Oxalobacteraceae* (phylum
418 *Proteobacteria*, class *Betaproteobacteria*, order *Burkholderiales*, 216 bp). To date,
419 many *Pseudomonas* strains in γ-*Proteobacteria* have been shown to possess the
420 capability of degrading aromatic hydrocarbons such as pyrene, phenanthrene,
421 naphthalene, toluene, and phenol in crude oil-contaminated soil (47).
422 *Burkholderiales*-related bacteria in β-*Proteobacteria* were also related to PAHs
423 removal, and the family *Oxalobacteraceae* was widely found in PCBs- and
424 PAHs-contaminated soils (40, 48). Huang reported that a cultivated bacterial strain
425 from the class *Burkholderiales* could degrade PAHs (41). However, no previous
426 studies using SIP have demonstrated the BaP-degradation capacity of
427 *Burkholderiales*-related bacteria, and our results in Mt. Baicaowa soils suggest such
428 possibilities.

429 The coupling of TRFLP with SIP enabled us to compare the TRFLP profiles over
430 a range of BDs for both ^{13}C-labeled and unlabeled samples at different time intervals
431 to avoid false-positive results. For example, in the M treatment, although three clones
432 with predicted 237-, 372-, and 215-bp *Hae*III cut sites were dominant in the 16S
433 rRNA clone library, and the corresponding TRFs constituted a high proportion in the

434 ^{13}C heavy fractions from ^{13}C-BaP-amended treatment, no significant difference was
435 observed in these TRFs between the ^{13}C-BaP and ^{12}C-BaP treatments, suggesting their
436 limited roles in *in situ* BaP degradation in our study.

437 The conflict between Gram-positive PAH-RHDα genes and detected
438 Gram-negative BaP degraders is a puzzle. Such evolutionary distant has been
439 explained previously as horizontal gene transfers of PAH-RHDα genes and other
440 genes between Gram-positive and Gram-negative bacteria (49-52). For instance, the
441 classical *nah*-like genes were shared among gram-negative bacteria (49). *aphA-3*, an
442 antibiotic resistance gene in *Campylobacter* encoding 3'-aminoglycoside
443 phosphotransferases modifying the structure of kanamycin, was transferred between
444 gram-positive and gram-negative bacteria (53). In our study, SIP results could not
445 directly affiliate the Gram-positive PAH-RHDα genes to the functional
446 Gram-negative host, therefore not able to prove the evidence of horizontal gene
447 transfer. Further work is suggested on the single-cell isolation and genome
448 amplification of individual BaP degraders (54) and deeper investigation on the
449 PAH-RHDα genes within the targeting functional species.

450 **Effects of salicylate on BaP degradation and community structure.** The
451 addition of salicylate significantly changed the functional microbial community
452 structure in the heavy fractions derived from the Mt. Baicaowa soils, but not the BaP
453 degradation. The dominant species shifted from *Rhodanobacter*-related bacteria in B
454 microcosm to *Burkholderiales*-related bacteria in BS treatment, although
455 *Acidobacteria*-related microorganisms existed in both treatments. The bacteria

456 capable of degrading BaP (*Burkholderiales*) in B and BS treatments were detected as
457 identical using DNA-SIP (Table S1). Nevertheless, the similar BaP removal efficiency
458 between B and BS treatments hinted that BaP degradation was not stimulated by the
459 functional microbial structure change and increasing *Burkholderiales*-related bacteria,
460 consistent with a previous study by Powell (12). Since small pH variation might
461 significantly affect the biodegradation of xenobiotics and other organic compounds in
462 oligotrophic environments (55), the possible reason was the decreased PAHs
463 degradation activity of dominant *Burkholderiales*-related bacteria under low pH
464 conditions (56), like pH=6.0 in Mt. Baicaowa soils.

465 However, the TRFLP in M and MS treatments suggested that the addition of
466 salicylate changed both functional microbial community structure in heavy fractions
467 and BaP degradation rate (Table S1). The dominant species correlated with BaP
468 degradation shifted from *Terrimonas* to *Oxalobacteraceae* after the salicylate addition.
469 The functional PAH-RHD genes might change (Fig. 3), and salicylate also accelerated
470 the BaP degradation in Mt. Maoer microcosms (Table 1). Previous studies showed a
471 significant increase in the rate of naphthalene mineralization in soil after enrichment
472 with salicylate spiking (38). The presence of phenanthrene and salicylate also greatly
473 enhanced the initial removal rates of benz[a]anthracene, chrysene, and
474 benzo[a]pyrene by *P. saccharophila* P15 (16). The addition of salicylate to
475 PAHs-contaminated soils was shown to increase the quantity of
476 naphthalene-degrading bacteria (57, 58), and stimulate the degradation of
477 benzo[a]anthracene, chrysene (16), fluoranthene (16, 17), and BaP (8, 16).

478 Salicylate was also reported to sustain populations of biological control bacteria with
479 naphthalene-degrading genes in agricultural systems (59), and various salicylate
480 additives (spiked or slow/continuous addition) have been used to select different
481 microbial communities (38).

482 The effects of salicylate on PAHs removal and functional microbial community
483 structure depend on the soil properties and the bacterial profiles in the soils. Although
484 salicylate is the central metabolite of many PAHs-degradation processes, it is not
485 associated with some pathways, and its stimulating effect, therefore, might not be
486 suitable for all cases of PAHs degradation. For example, the addition of salicylate had
487 no effect on phenanthrene or pyrene removal in PAHs-contaminated soils (60). After
488 enrichment with salicylate, the initial naphthalene mineralization rate rather than
489 phenanthrene and BaP, was enhanced by the microbial community in a bioreactor for
490 a PAHs-contaminated soil treatment (38). While, in uncontaminated soils, salicylate
491 only improved pyrene removal but did not affect BaP (60), which may explain why
492 salicylate stimulated BaP removal in Mt. Maoer soils, but not Mt. Baicaowa.

493 In summary, three phylotypes in two different forest soils were linked with BaP
494 degradation using the culture-independent SIP technique. The addition of salicylate
495 affected the bacteria correlated with BaP metabolism and the BaP degradation
496 efficiency differently in the two forest soils. Besides, a new PAH-RHDα gene
497 involved in BaP metabolism was detected in the salicylate-amended soils from Mt.
498 Maoer. Our results provide a deeper understanding of the contribution of SIP to
499 identifying the functions of uncultured microorganisms, expand our knowledge on

500 bacteria possessing the ability of BaP mineralization, and reveal specific effects of
501 salicylate on the BaP-biodegradation process.
502
503 **ACKNOWLEDGEMENT**

504 This study was supported by the Joint Funds of the National Natural Science
505 Foundation of China and the Natural Science Foundation of Guangdong Province,
506 China (No. U1133004), the National Natural Science Foundation of China (Nos.
507 41173082 & 41322008), and the Scientific and Technological Planning Project of
508 Guangzhou, China (No. 201510010038).
509
510

511 # REFERENCE

512 1. **Baek SO, Field RA, Goldstone ME, Kirk PW, Lester JN, Perry R.** 1991. A Review of Atmospheric
513 Polycyclic Aromatic-Hydrocarbons - Sources, Fate and Behavior. Water Air Soil Poll **60:**279-300.
514 2. **Zhang YX, Tao S.** 2009. Global atmospheric emission inventory of polycyclic aromatic
515 hydrocarbons (PAHs) for 2004. Atmos Environ **43:**812-819.
516 3. **Keith LH, Telliard WA.** 1979. Priority Pollutants I-a Perspective View. Environ Sci Technol
517 **13:**416-423.
518 4. **Rodriguez-Fragoso L, Melendez K, Hudson LG, Lauer FT, Burchiel SW.** 2009. EGF-receptor
519 phosphorylation and downstream signaling are activated by benzo[a]pyrene 3,6-quinone and
520 benzo[a]pyrene 1,6-quinone in human mammary epithelial cells. Toxicol Appl Pharm
521 **235:**321-328.
522 5. **Wills LP, Zhu SQ, Willett KL, Di Giulio RT.** 2009. Effect of CYP1A inhibition on the
523 biotransformation of benzo[a]pyrene in two populations of Fundulus heteroclitus with different
524 exposure histories. Aquat Toxicol **92:**195-201.
525 6. **Anonymous.** 2010. Iarc Monographs on the Evaluation of Carcinogenic Risks to Humans. Iarc
526 Monog Eval Carc **95:**9-38.
527 7. **Juhasz AL, Naidu R.** 2000. Bioremediation of high molecular weight polycyclic aromatic
528 hydrocarbons: a review of the microbial degradation of benzo[a]pyrene. Int Biodeter Biodegr
529 **45:**57-88.
530 8. **Rentz JA, Alvarez PJJ, Schnoor JL.** 2008. Benzo[a]pyrene degradation by Sphingomonas
531 yanoikuyae JAR02. Environ Pollut **151:**669-677.
532 9. **Peng H, Yin H, Deng J, Ye JS, Chen SN, He BY, Zhang N.** 2012. Biodegradation of Benzo[a]pyrene
533 by Arthrobacter oxydans B4. Pedosphere **22:**554-561.
534 10. **Mishra S, Singh SN.** 2014. Biodegradation of benzo(a)pyrene mediated by catabolic enzymes of
535 bacteria. Int J Environ Sci Te **11:**1571-1580.
536 11. **Jurelevicius D, Alvarez VM, Peixoto R, Rosado AS, Seldin L.** 2012. Bacterial polycyclic aromatic
537 hydrocarbon ring-hydroxylating dioxygenases (PAH-RHD) encoding genes in different soils from
538 King George Bay, Antarctic Peninsula. Appl Soil Ecol **55:**1-9.
539 12. **Cebron A, Norini MP, Beguiristain T, Leyval C.** 2008. Real-Time PCR quantification of PAH-ring
540 hydroxylating dioxygenase (PAH-RHD alpha) genes from Gram positive and Gram negative
541 bacteria in soil and sediment samples. J Microbiol Meth **73:**148-159.
542 13. **Lily MK, Bahuguna A, Dangwal K, Garg V.** 2009. Degradation of Benzo [a] Pyrene by a Novel
543 Strain Bacillus Subtilis Bmt4i (Mtcc 9447). Braz J Microbiol **40:**884-892.
544 14. **Kanaly RA, Harayama S.** 2000. Biodegradation of high-molecular-weight polycyclic aromatic
545 hydrocarbons by bacteria. J Bacteriol **182:**2059-2067.
546 15. **Kanaly RA, Harayama S.** 2010. Advances in the field of high-molecular-weight polycyclic aromatic
547 hydrocarbon biodegradation by bacteria. Microb Biotechnol **3:**136-164.
548 16. **Chen SH, Aitken MD.** 1999. Salicylate stimulates the degradation of high molecular weight
549 polycyclic aromatic hydrocarbons by Pseudomonas saccharophila P15. Environ Sci Technol
550 **33:**435-439.
551 17. **Alemayehu D, Gordon LM, O'Mahony MM, O'Leary ND, Dobson ADW.** 2004. Cloning and
552 functional analysis gene involved in indigo production by gene disruption of a novel and
553 fluoranthene metabolism in Pseudomonas alcaligenes PA-10. Fems Microbiol Lett **239:**285-293.

554 18. **Bode HB, Muller R.** 2005. The impact of bacterial genomics on natural product research. Angew
555 Chem Int Edit **44:**6828-6846.
556 19. **Galvao TC, Mohn WW, de Lorenzo V.** 2005. Exploring the microbial biodegradation and
557 biotransformation gene pool. Trends Biotechnol **23:**497-506.
558 20. **Lorenz P, Eck J.** 2005. Metagenomics and industrial applications. Nat Rev Microbiol **3:**510-516.
559 21. **Oren A.** 2004. Prokaryote diversity and taxonomy: current status and future challenges. Philos T
560 Roy Soc B **359:**623-638.
561 22. **Radajewski S, Ineson P, Parekh NR, Murrell JC.** 2000. Stable-isotope probing as a tool in
562 microbial ecology. Nature **403:**646-649.
563 23. **Singleton DR, Sangaiah R, Gold A, Ball LM, Aitken MD.** 2006. Identification and quantification of
564 uncultivated Proteobacteria associated with pyrene degradation in a bioreactor treating
565 PAH-contaminated soil. Environ Microbiol **8:**1736-1745.
566 24. **Luo CL, Xie SG, Sun WM, Li XD, Cupples AM.** 2009. Identification of a Novel Toluene-Degrading
567 Bacterium from the Candidate Phylum TM7, as Determined by DNA Stable Isotope Probing. Appl
568 Environ Microb **75:**4644-4647.
569 25. **Gutierrez T, Singleton DR, Aitken MD, Semple KT.** 2011. Stable Isotope Probing of an Algal
570 Bloom To Identify Uncultivated Members of the Rhodobacteraceae Associated with
571 Low-Molecular-Weight Polycyclic Aromatic Hydrocarbon Degradation. Appl Environ Microb
572 **77:**7856-7860.
573 26. **Singleton DR, Powell SN, Sangaiah R, Gold A, Ball LM, Aitken MD.** 2005. Stable-isotope probing
574 of bacteria capable of degrading salicylate, naphthalene, or phenanthrene in a Bioreactor
575 treating contaminated soil. Appl Environ Microb **71:**1202-1209.
576 27. **Zhang SY, Wang QF, Xie SG.** 2012. Stable isotope probing identifies anthracene degraders under
577 methanogenic conditions. Biodegradation **23:**221-230.
578 28. **Peng JJ, Zhang Y, Su JQ, Qiu QF, Jia ZJ, Zhu YG.** 2013. Bacterial communities predominant in the
579 degradation of C-13(4)-4,5,9,10-pyrene during composting. Bioresource Technol **143:**608-614.
580 29. **Jones MD, Crandell DW, Singleton DR, Aitken MD.** 2011. Stable-isotope probing of the polycyclic
581 aromatic hydrocarbon-degrading bacterial guild in a contaminated soil. Environ Microbiol
582 **13:**2623-2632.
583 30. **Sul WJ, Park J, Quensen JF, Rodrigues JLM, Seliger L, Tsoi TV, Zylstra GJ, Tiedje JM.** 2009.
584 DNA-Stable Isotope Probing Integrated with Metagenomics for Retrieval of Biphenyl Dioxygenase
585 Genes from Polychlorinated Biphenyl-Contaminated River Sediment. Appl Environ Microb
586 **75:**5501-5506.
587 31. **Uhlik O, Wald J, Strejcek M, Musilova L, Ridl J, Hroudova M, Vlcek C, Cardenas E, Mackova M,**
588 **Macek T.** 2012. Identification of Bacteria Utilizing Biphenyl, Benzoate, and Naphthalene in
589 Long-Term Contaminated Soil. Plos One **7**.
590 32. **Mu DY, Scow KM.** 1994. Effect of Trichloroethylene (Tce) and Toluene Concentrations on Tce and
591 Toluene Biodegradation and the Population-Density of Tce and Toluene Degraders in Soil. Appl
592 Environ Microb **60:**2661-2665.
593 33. **Sun WM, Xie SG, Luo CL, Cupples AM.** 2010. Direct Link between Toluene Degradation in
594 Contaminated-Site Microcosms and a Polaromonas Strain. Appl Environ Microb **76:**956-959.
595 34. **Cupples AM, Sims GK.** 2007. Identification of in situ 2,4-dichlorophenoxyacetic acid-degrading
596 soil microorganisms using DNA-stable isotope probing. Soil Biol Biochem **39:**232-238.
597 35. **Sun WM, Cupples AM.** 2012. Diversity of Five Anaerobic Toluene-Degrading Microbial

598 Communities Investigated Using Stable Isotope Probing. Appl Environ Microb **78:**972-980.
599 36. **Warshawsky D, Ladow K, Schneider J.** 2007. Enhanced degradation of benzo[a]pyrene by
600 Mycobacterium sp in conjunction with green alga. Chemosphere **69:**500-506.
601 37. **Moody JD, Freeman JP, Fu PP, Cerniglia CE.** 2004. Degradation of benzo[a]pyrene by
602 Mycobacterium vanbaalenii PYR-1. Appl Environ Microb **70:**340-345.
603 38. **Powell SN, Singleton DR, Aitken MD.** 2008. Effects of enrichment with salicylate on bacterial
604 selection and PAH mineralization in a microbial community from a bioreactor treating
605 contaminated soil. Environ Sci Technol **42:**4099-4105.
606 39. **Ang EL, Zhao HM, Obbard JP.** 2005. Recent advances in the bioremediation of persistent organic
607 pollutants via biomolecular engineering. Enzyme Microb Tech **37:**487-496.
608 40. **de Carcer DA, Martin M, Karlson U, Rivilla R.** 2007. Changes in bacterial populations and in
609 biphenyl dioxygenase gene diversity in a polychlorinated biphenyl-polluted soil after introduction
610 of willow trees for rhizoremediation. Appl Environ Microb **73:**6224-6232.
611 41. **Huang X, Luo Y, Hu Z, Tian Y.** 2006. Recent advance in the study of persistent organic pollutants
612 bioremediation. Acta Sci Circum **26:**353-361.
613 42. **Juhasz AL, Britz ML, Stanley GA.** 1997. Degradation of benzo[a]pyrene, dibenz[a,h]anthracene
614 and coronene by Burkholderia cepacia. Water Sci Technol **36:**45-51.
615 43. **Zafra G, Absalon AE, Cuevas MD, Cortes-Espinosa DV.** 2014. Isolation and Selection of a Highly
616 Tolerant Microbial Consortium with Potential for PAH Biodegradation from Heavy Crude
617 Oil-Contaminated Soils. Water Air Soil Poll **225**.
618 44. **Yoon MH, Im WT.** 2007. Flavisolibacter ginsengiterrae gen. nov., sp nov and Flavisolibacter
619 ginsengisoli sp nov., isolated from ginseng cultivating soil. Int J Syst Evol Micr **57:**1834-1839.
620 45. **Ye DY, Siddiqi MA, Maccubbin AE, Kumar S, Sikka HC.** 1996. Degradation of polynuclear
621 aromatic hydrocarbons by Sphingomonas paucimobilis. Environ Sci Technol **30:**136-142.
622 46. **Everard A, Lazarevic V, Derrien M, Girard M, Muccioli GG, Neyrinck AM, Possemiers S, Van
623 Holle A, Francois P, de Vos WM, Delzenne NM, Schrenzel J, Cani PD.** 2011. Responses of gut
624 microbiota and glucose and lipid metabolism to prebiotics in genetic obese and diet-induced
625 leptin-resistant mice. Diabetes **60:**3307-3307.
626 47. **Chang. H, Nie. M, Ge. B, Liu. C, Yang. Q, Zhou. L, Fan. X, Sun. C.** 2013. Effects of rhamnolipid on
627 oil degradation by Pseudomonas aeruginosa strain NY3. Chin J Environ Eng **7:**771-776.
628 48. **Tejeda-Agredano MC, Gallego S, Vila J, Grifoll M, Ortega-Calvo JJ, Cantos M.** 2013. Influence of
629 the sunflower rhizosphere on the biodegradation of PAHs in soil. Soil Biol Biochem **57:**830-840.
630 49. **Habe H, Omori T.** 2003. Genetics of polycyclic aromatic hydrocarbon metabolism in diverse
631 aerobic bacteria. Biosci Biotech Bioch **67:**225-243.
632 50. **Herrick JB, StuartKeil KG, Ghiorse WC, Madsen EL.** 1997. Natural horizontal transfer of a
633 naphthalene dioxygenase gene between bacteria native to a coal tar-contaminated field site.
634 Appl Environ Microb **63:**2330-2337.
635 51. **Wilson MS, Herrick JB, Jeon CO, Hinman DE, Madsen EL.** 2003. Horizontal transfer of phnAc
636 dioxygenase genes within one of two phenotypically and genotypically distinctive
637 naphthalene-degrading guilds from adjacent soil environments. Appl Environ Microb
638 **69:**2172-2181.
639 52. **Yagi JM, Sims D, Brettin T, Bruce D, Madsen EL.** 2009. The genome of Polaromonas
640 naphthalenivorans strain CJ2, isolated from coal tar-contaminated sediment, reveals
641 physiological and metabolic versatility and evolution through extensive horizontal gene transfer.

642 Environ Microbiol **11:**2253-2270.
643 53. **Trieucuot P, Gerbaud G, Lambert T, Courvalin P.** 1985. Invivo Transfer of Genetic Information
644 between Gram-Positive and Gram-Negative Bacteria. Embo J **4:**3583-3587.
645 54. **Zhang DY, Berry JP, Zhu D, Wang Y, Chen Y, Jiang B, Huang S, Langford H, Li GH, Davison PA, Xu**
646 **J, Aries E, Huang WE.** 2015. Magnetic nanoparticle-mediated isolation of functional bacteria in a
647 complex microbial community. Isme J **9:**603-614.
648 55. **Kastner M, Breuer-Jammali M, Mahro B.** 1998. Impact of inoculation protocols, salinity, and pH
649 on the degradation of polycyclic aromatic hydrocarbons (PAHs) and survival of PAH-degrading
650 bacteria introduced into soil. Appl Environ Microb **64:**359-362.
651 56. **Wong JWC, Lai KM, Wan CK, Ma KK, Fang M.** 2002. Isolation and optimization of
652 PAH-degradative bacteria from contaminated soil for PAHs bioremediation. Water Air Soil Poll
653 **139:**1-13.
654 57. **Ogunseitan OA, Delgado IL, Tsai YL, Olson BH.** 1991. Effect of 2-Hydroxybenzoate on the
655 Maintenance of Naphthalene-Degrading Pseudomonads in Seeded and Unseeded Soil. Appl
656 Environ Microb **57:**2873-2879.
657 58. **Ogunseitan OA, Olson BH.** 1993. Effect of 2-Hydroxybenzoate on the Rate of Naphthalene
658 Mineralization in Soil. Appl Microbiol Biot **38:**799-807.
659 59. **Ji PS, Wilson M.** 2003. Enhancement of population size of a biological control agent and efficacy
660 in control of bacterial speck of tomato through salicylate and ammonium sulfate amendments.
661 Appl Environ Microb **69:**1290-1294.
662 60. **Carmichael LM, Pfaender FK.** 1997. The effect of inorganic and organic supplements on the
663 microbial degradation of phenanthrene and pyrene in soils. Biodegradation **8:**1-13.
664
665

666

667 **FIGURE AND TABLE LEGENDS**

668 **Table**

669 **Table 1.** Percentage of BaP remaining in soils over time

670 **Figures**

671 **Fig. 1** Relative abundance of TRFLP fragments (digested by HaeIII) assigned to *Burkholderia1*

672 (A), *Burkholderia2* (B), *Terrimonas* (C), *Oxalobacteraceae* (D) against the buoyant density

673 gradients in B, BS, M and MS treatments.

674 **Fig. 2** Phylogenetic tree of PAH-RHDα-M genes from MS (microcosms from Mt. Maoer soil

675 amended with salicylate) and M (microcosms from Mt. Maoer soil without salicylate) treatments

676 along with the closest matches in GenBank, constructed with MEGA 5.0 software using the

677 neighbor-joining method.

678 **Fig. 3** PAH-RHDα-M gene copies in ultracentrifugation fractions from ^{13}C-BaP and ^{12}C-BaP

679 amended microcosms determined by qPCR. A and B represent the microcosms from Mt. Maoer

680 soil with/without salicylate addition. Figure symbols: □ ^{13}C-BaP (~52% BaP degraded); ■

681 ^{12}C-BaP (~42% BaP degraded).

682 **Table 1.** Percentage of BaP remaining in soils over time

Time (days)	B(%)			BS(%)			M(%)			MS(%)		
	^{12}C-NB	^{12}C-BT	^{13}C-BT	^{12}C-NB	^{12}C-BT	^{13}C-BT	^{12}C-NB	^{12}C-BT	^{13}C-BT	^{12}C-NB	^{12}C-BT	^{13}C-BT
7	87.1	70.5	71.3	85.3	67.2	66.3	-	-	-	-	-	-
14	78.4	53.5	52.7	83.1	60.1	62.1	88.9	56.8	59.7	72.9	25.6	24.8
28	80.6	47.2	48.6	72.6	41.5	41.5	82.0	38.3	37.9	70.4	17.9	18.2
42	-	-	-	-	-	-	81.0	35.4	36.4	69.7	13.9	11.7

683 Note: ^{12}C-NB represents the non-bioactive autoclaved treatment; ^{12}C-BT represents the treatment with ^{12}C-BaP as the sole carbon sources; ^{13}C-BT represents the treatment
684 with ^{13}C-BaP as the sole carbon sources. B and BS represent the soil microcosms from Mt. Baicaowa amended without/with salicylate, whereas M and MS refer to the
685 soil microcosms from Mountain Maoer amended without/with salicylate. " - " means samples were not set at the time.

686

687

688

689

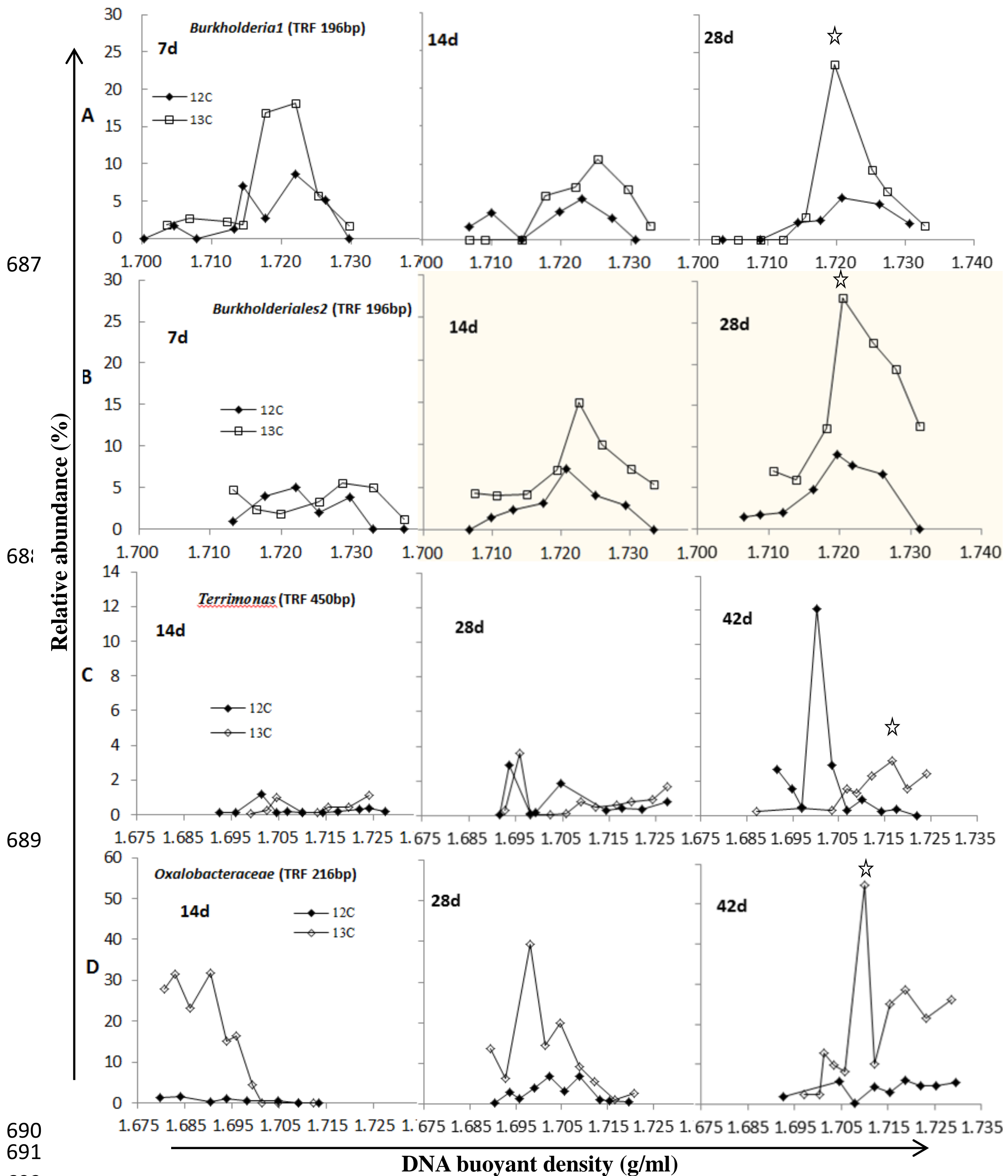

690
691
692
693 **Fig. 1.** Relative abundance of TRFLP fragments (digested by HaeIII) assigned to *Burkholderia1*
694 (A), *Burkholderia2* (B), *Terrimonas* (C), *Oxalobacteraceae* (D) against the buoyant density
695 gradients in B, BS, M and MS treatments. The bacterial DNA were extracted from B (microcosms
696 from Mt. Baicaowa soil) and BS (microcosms from Mt. Baicaowa soil amended with salicylate)
697 after 7, 14 and 28 days, and M (microcosms from Mt. Maoer soil) and MS (microcosms from Mt.
698 Maoer soil amended with salicylate) after 14, 28 and 42 days. Figure symbols: □ ^{13}C-BaP; ■
699 ^{12}C-BaP. ☆ shows the fractions used for sequencing of partial PAH-RHDα and 16S rRNA genes
700 involved in BaP degradation in all the treatments.

701

702

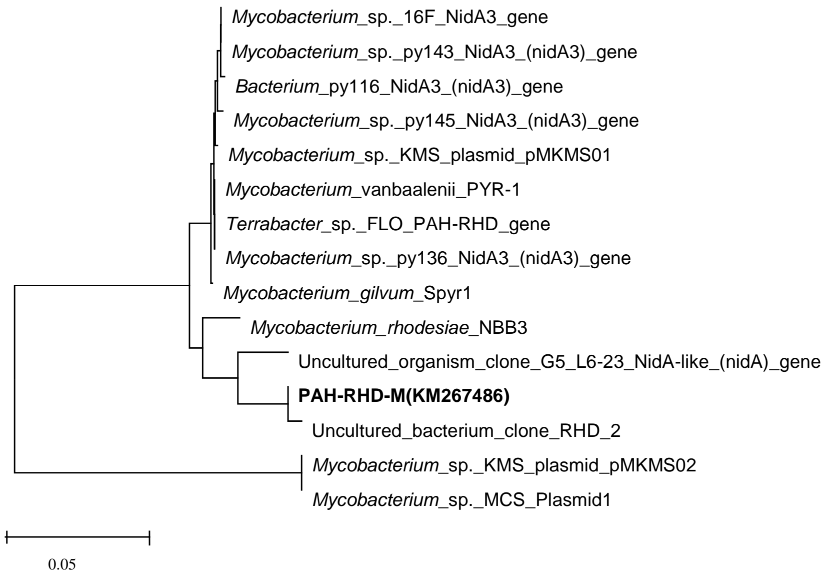

703

704 **Fig. 2.** Phylogenetic tree of PAH-RHDα-M genes from MS (microcosms from Mt. Maoer soil
705 amended with salicylate) and M (microcosms from Mt. Maoer soil without salicylate) treatments
706 along with the closest matches in GenBank, constructed with MEGA 5.0 software using the
707 neighbor-joining method.

708

709
710
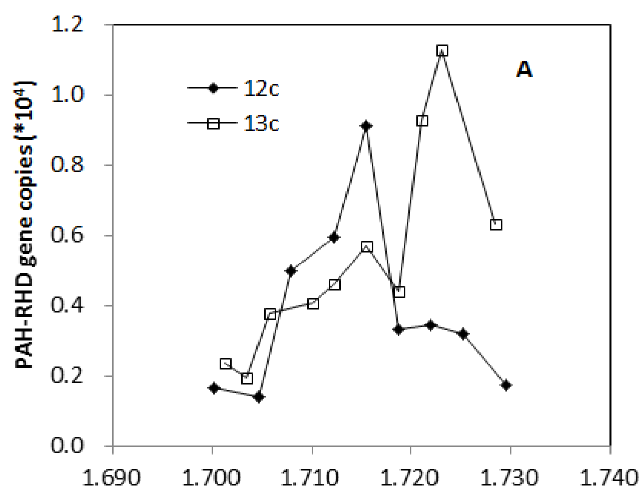

711
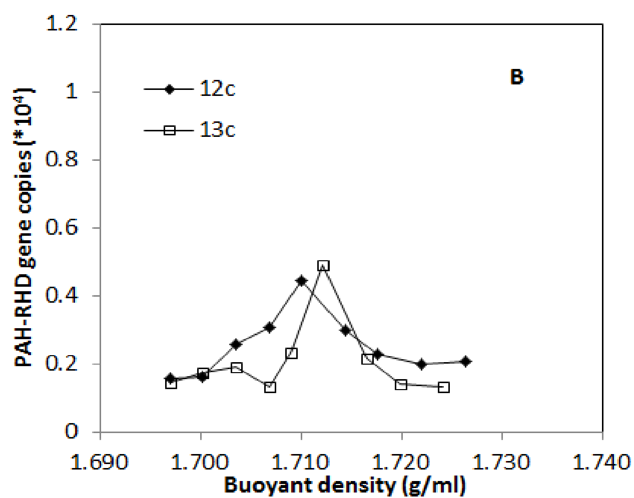

712
713 **Fig. 3.** PAH-RHDα-M gene copies in ultracentrifugation fractions from ^{13}C-BaP and ^{12}C-BaP
714 amended microcosms determined by qPCR. A and B represent the microcosms from Mt. Maoer
715 soil with/without salicylate addition. Figure symbols: □ ^{13}C-BaP (~52% BaP degraded); ■
716 ^{12}C-BaP (~42% BaP degraded).
717
718
719
720
721
722